Opsins in Onychophora (Velvet Worms) Suggest a Single Origin and Subsequent Diversification of Visual Pigments in Arthropods

Lars Hering,*[1] Miriam J. Henze,[2] Martin Kohler,[2] Almut Kelber,[2] Christoph Bleidorn,[3] Maren Leschke,[1] Birgit Nickel,[4] Matthias Meyer,[4] Martin Kircher,[4,5] Paul Sunnucks,[6] and Georg Mayer[1]

[1]Animal Evolution and Development, Institute of Biology, University of Leipzig, Leipzig, Germany

[2]Department of Biology, Lund University, Lund, Sweden

[3]Molecular Evolution and Systematics of Animals, Institute of Biology, University of Leipzig, Leipzig, Germany

[4]Department of Evolutionary Genetics, Max Planck Institute for Evolutionary Anthropology, Leipzig, Germany

[5]Department of Genome Sciences, University of Washington

[6]Australian Centre for Biodiversity and School of Biological Sciences, Monash University, Melbourne, Victoria, Australia

*Corresponding author: E-mail: lars.hering@uni-leipzig.de.

Associate editor: Adriana Briscoe

Abstract

Multiple visual pigments, prerequisites for color vision, are found in arthropods, but the evolutionary origin of their diversity remains obscure. In this study, we explore the opsin genes in five distantly related species of Onychophora, using deep transcriptome sequencing and screening approaches. Surprisingly, our data reveal the presence of only one opsin gene (onychopsin) in each onychophoran species, and our behavioral experiments indicate a maximum sensitivity of onychopsin to blue–green light. In our phylogenetic analyses, the onychopsins represent the sister group to the monophyletic clade of visual r-opsins of arthropods. These results concur with phylogenomic support for the sister-group status of the Onychophora and Arthropoda and provide evidence for monochromatic vision in velvet worms and in the last common ancestor of Onychophora and Arthropoda. We conclude that the diversification of visual pigments and color vision evolved in arthropods, along with the evolution of compound eyes—one of the most sophisticated visual systems known.

Key words: vision, opsin evolution, Arthropoda, Panarthropoda, compound eyes.

Introduction

Opsins are specialized proteins that play a major role in animal vision (Shichida and Imai 1998; Shichida and Matsuyama 2009; review Porter et al. 2012). Evolutionary changes in protein structure may affect the photosensitivity of visual pigments to different wavelengths, thus altering visual perception. Monochromatic vision is present when only one opsin molecule is involved, whereas multiple visual pigments are necessary for color vision (Shichida and Imai 1998; Briscoe and Chittka 2001). Color vision has been reported from two distantly related major animal groups: vertebrates and arthropods. Although vertebrates and arthropods have inherited ciliary opsins (c-opsins) and rhabdomeric opsins (r-opsins) from their last common ancestor, vertebrates mainly use c-opsins in the photoreceptors of their eyes, whereas arthropods use r-opsins (Arendt and Wittbrodt 2001; Arendt 2003; Plachetzki et al. 2007; Vopalensky and Kozmik 2009).

Previous studies revealed a remarkable diversity of r-opsins among arthropods (e.g., Briscoe 2000; Porter et al. 2007; Koyanagi et al. 2008; Kashiyama et al. 2009; Katti et al. 2010). These comprise up to four paralogous groups characterized by their sensitivity to different wavelengths of light, including long (green–yellow), middle (blue–green), short (blue), and ultraviolet wavelengths. The phylogenetic origin of these paralogous groups remains uncertain as they might have evolved from a single ancestral arthropod visual opsin gene (Plachetzki et al. 2007) or, alternatively, their divergence might have preceded the evolution of arthropods (Koyanagi et al. 2008; Kashiyama et al. 2009). To decide between these two alternative hypotheses and to clarify the evolution of visual pigments in arthropods, we identified and analyzed the functional opsins in Onychophora, which recent, comprehensive, phylogenomic studies place as the sister group of Arthropoda (Campbell et al. 2011; Edgecombe et al. 2011). In addition, we carried out behavioral experiments to explore the response to light in these animals, which might have retained the ancestral type of visual organs when compared with arthropods (Mayer 2006).

In contrast to most arthropods, which show two visual systems (median ocelli and compound eyes), onychophorans bear only one pair of ocellus-like structures resembling the eyes of Early Cambrian lobopodians (Mayer 2006; Schoenemann et al. 2009). Notably, the onychophoran eyes are simple structures that are innervated by the central part of the brain, although they lie laterally on the head (Mayer 2006;

Strausfeld, Strausfeld, Loesel, et al. 2006; Strausfeld, Strausfeld, Stowe, et al. 2006). The structure, development, and innervation pattern of the onychophoran eyes suggest that they are homologous to the median ocelli rather than to the compound eyes of arthropods (Mayer 2006; Schoenemann et al. 2009; Lehmann et al. 2012; but see Ma et al. 2012 for an opposed view). Thus, the study of opsin genes in these visual organs might shed light on the evolutionary history of vision in arthropods.

Materials and Methods

Library Preparation and Sequencing Procedure

Specimens of five onychophoran species, including three species of Peripatopsidae (*Euperipatoides rowelli, Phallocephale tallagandensis,* and *Ooperipatus hispidus*) and two species of Peripatidae (*Epiperipatus* cf. *isthmicola,* and *Eoperipatus* sp.) were obtained as described by Baer and Mayer (2012). Total RNA was extracted separately from different tissues, including eyes, heads, entire specimens, and different embryonic stages, using the TRIzol® Reagent (Invitrogen, Carlsbad, CA) and the RNeasy MinElute Cleanup Kit (Qiagen, Hilden, Germany) according to the manufacturer's protocols. Double-stranded complementary DNA was prepared following Illumina's messenger RNA (mRNA)-seq sample preparation guide (Part #1004898 Rev. D). Briefly, mRNA was isolated from total RNA using Dynal oligo(dT) beads (Invitrogen) and fragmented (ca., 200 bp) using divalent cationic ions. First-strand synthesis was performed with random hexamer primers, using Superscript II polymerase (Invitrogen). Subsequent second-strand synthesis was carried out with DNA Pol I polymerase (Invitrogen). Starting at the blunt end repair step, multiplex sequencing libraries were prepared following the multiplex protocol of Meyer and Kircher (2010), with modifications for double indexing described in Kircher et al. (2012). These libraries were sequenced according to the manufacturer's instructions for single-read multiplex experiments with 76 cycles paired end on the Genome Analyzer IIx platform (v4 sequencing chemistry and v4 cluster generation kit; Illumina, San Diego, CA). A second index read was performed as described in Kircher et al. (2012). Raw sequences were analyzed with IBIS 1.1.2 (Kircher et al. 2009). For highly accurate sample identification, sequences with falsely paired indexes were discarded. Paired-end reads from a single cluster were merged, if at least 11 bp were overlapping (Kircher et al. 2011). Reads with low complexity were removed. As it has been shown that read quality can have a strong impact on sequence assemblies (Minoche et al. 2011; Salzberg et al. 2012), we used different filtering strategies for our raw data. For each library from the five species, we trimmed the Illumina raw data at three different levels of stringency (Filter15: reads with more than five bases below a quality score of 15 were removed; Filter30: reads with less than 20 bases in a row with a quality score of at least 30 were removed; Filter25: same as Filter30 but the threshold value was set to 25 to keep as many high-quality reads as possible, 63–89% compared with Filter15). This was done to deal with the tradeoff between the quality and quantity of reads as we lost many reads (51–90% compared with Filter15) by using the very stringent Filter30, which thus might have led to a loss of lowly expressed genes (supplementary table S1, Supplementary Material online). The distribution of average read quality scores and the base-quality distribution among the base positions for each filter and library indicate an increasing quality with trim stringency (supplementary figs. S1 and S2, Supplementary Material online). For all libraries and filters described, sequence reads were assembled de novo using the CLC Genomics Workbench 5.1 (CLC bio, Aarhus, Denmark) with the following parameters: mismatch cost 3; insertion cost 3; deletion cost 3; length fraction 0.5; similarity fraction 0.8; minimum contig length 200; automatic word size; automatic bubble size; and contig adjustment by mapped reads (supplementary table S1, Supplementary Material online).

Extensive Basic Local Alignment Search Tool/HMMER Searches for Candidate Contigs

Two different approaches were used to search for candidate contigs in the assemblies (fig. 1). First, tBLASTn/BLASTP searches (Altschul et al. 1997) of 20 representatives from each major clade of opsins were performed, including the five onychopsins as reciprocal BLAST searches. All hits with an e value ≤ 1e-20 were stored (335 hits in total). Second, the software package HMMER v3.0 (http://hmmer.org) was used to scan for additional candidates. Therefore, we built hmmprofiles for each of the eight major clades of opsins (cnidopsins, vertebrate c-opsins, arthropod pteropsins, Group 4 opsins, arthropsins, melanopsins, nonarthropod r-opsins, and arthropod visual r-opsins), plus onychopsins (for GenBank accession numbers for BLAST reference sequences and for accession numbers of references used to build hmmprofiles, see supplementary table S2, Supplementary Material online). All HMMER hits with an e value ≤ 1e-30 (470 hits in total), and all BLAST hits recovered as described above were used for further analyses. After removing redundant hits, 98 unique contigs were used as a query for reciprocal BLAST searches against the nr/nt database of GenBank, and the best hit for each query sequence was stored (38 unique GenBank entries). These 38 unique GenBank hits, the 98 unique candidate contigs from the onychophoran transcriptomes, and all references used as queries for the initial BLAST searches and to build the hmmprofiles were aligned with MAFFT (Katoh et al. 2002) (253 sequences in total; supplementary table S2, Supplementary Material online) and a maximum likelihood analysis was performed using RAxML v7.2.8 (Stamatakis 2006) to reveal the phylogenetic position of each candidate contig (supplementary fig. S3, Supplementary Material online).

Phylogenetic Analyses

The amino acid sequences of the onychopsins (GenBank: JN661372, JN661373, JQ780371, JQ780372 and JQ780373) were aligned with 251 representative sequences of visual and nonvisual opsins from other bilaterian taxa and G-protein-coupled receptor sequences other than opsins,
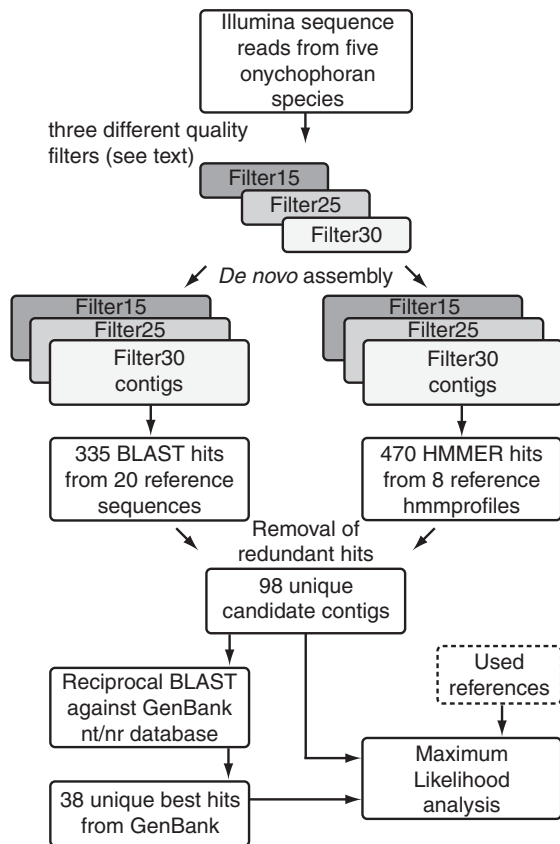
Fig. 1. Outline of the search pipeline used in this study to identify putative opsin genes in our datasets. We used BLAST (Altschul et al. 1997), HMMER v3.0 (http://hmmer.org), and customized Perl scripts (for reference sequences, see supplementary table S2, Supplementary Material online).

which are commonly used as outgroups in studies of opsin evolution (e.g., Porter et al. 2007; Suga et al. 2008; Passamaneck et al. 2011; Porter et al. 2012), using the FFT-NS-i option in MAFFT (Katoh et al. 2002). The alignment is available on request. ProtTest3 (Darriba et al. 2011) was applied to select the best-fit model of protein evolution (LG+I+G+F) according to the Akaike Information Criterion (AIC; Akaike 1973). The Pthread-Version of RAxML v7.2.8 (Stamatakis 2006) was used to infer the maximum likelihood tree (fig. 2 and supplementary fig. S4, Supplementary Material online). Bootstrap support values were estimated from 1,000 replicates. Bayesian inference analyses were performed using MrBayes 3.1.2 (Ronquist and Huelsenbeck 2003) with two independent runs of 5,000,000 generations and four chains each. As the LG model is unavailable in MrBayes 3.1.2, we used the next best-fit model (WAG+I+G) according to AIC derived by ProtTest3. Trees were sampled every 100 generations. After convergence of chains, indicated by deviation of split frequencies below 5%, we discarded the first 15,050 trees as burn-in. The remaining 34,951 trees were used to calculate a 50% majority rule consensus tree. The frequency at which a clade occurred among this sampling of trees was interpreted as its posterior probability (fig. 2 and supplementary fig. S5, Supplementary Material online). All phylogenetic trees were visualized and edited with iTOL (Letunic and Bork 2011).

Animals in Behavioral Experiments

Male specimens of *Epiperipatus* cf. *isthmicola* (Onychophora, Peripatidae) were maintained at 24°C under a 14 h:10 h light–dark cycle with a 30 min dawn and dusk period. Eleven specimens of 3.5–6 cm body length (head to tail) were tested during their night period. All of them were kept in the dark for at least 30 min before an experiment started.

Spectral Sensitivity of Negative Phototaxis

Tests were performed in darkness in a circular arena with a diameter of 45 cm and a circular wall (12 cm in height) covered with black velvet. The floor of the arena was made of matt laminated black paper with concentric red circles (fig. 3A). An infrared floodlight illuminated the scene for an infrared-sensitive camera (Sony HDR-CX11E, equipped with a Kenko Wide Conversion Lens 0.42x KCW-042) mounted 58 cm above the center of the arena. Quasi-monochromatic stimuli were produced by passing bright white light of a 450 W xenon arc lamp through one of six narrowband interference filters (Balzers AG) transmitting ultraviolet (363 nm center wavelength, 17 nm bandwidth at half maximum), blue (437 nm, 9 nm), green (550 nm, 9 nm), yellow (586 nm, 11 nm), orange (624, 8 nm) and red wavelengths (664 nm, 12 nm), respectively. The light beam was focused into a flexible UV-VIS-transmitting light guide, the far end of which was positioned at an angle of 56° on the rim of the arena. It provided an elliptical light spot of 9×11 cm diameter on and in front of the animal when a shutter was opened (fig. 3A and supplementary movie S1, Supplementary Material online). The intensity of the stimulus was adjusted by neutral density filters (Balzers AG), so that the number of quanta at the position of the head of the animal was 10^{13} quanta $cm^{-2} s^{-2}$ for all wavelengths.

An individual was placed in the center of the arena in a container. When the lid was lifted, the animal was allowed to walk into any direction. As soon as it crossed the circle of 15 cm diameter, the light stimulus of one of six wavelengths was turned on. No light stimulus was presented in the control trials. After each trial, the floor of the arena was rinsed to eliminate any chemical trail possibly left by an animal.

Based on the video sequences filmed with the infrared-sensitive camera, the walking path of each individual was reconstructed using its head as a reference. The strength of negative phototaxis was measured as the absolute angular difference between the walking direction over 2.5 cm before and after stimulus onset (arrowed white arc in fig. 3A). Runs in which animals turned anticlockwise were mirrored on the 0°–180° axis, resulting in apparent clockwise turns for all animals. Following the recommendation of Batschelet (1981) for the analyses of angular deviations ranging from 0° to 180°, linear statistics were used to evaluate the data.

Extraocular Photosensitivity

Animals were tested using the setup described above without filters in the light path. In darkness, an individual was placed
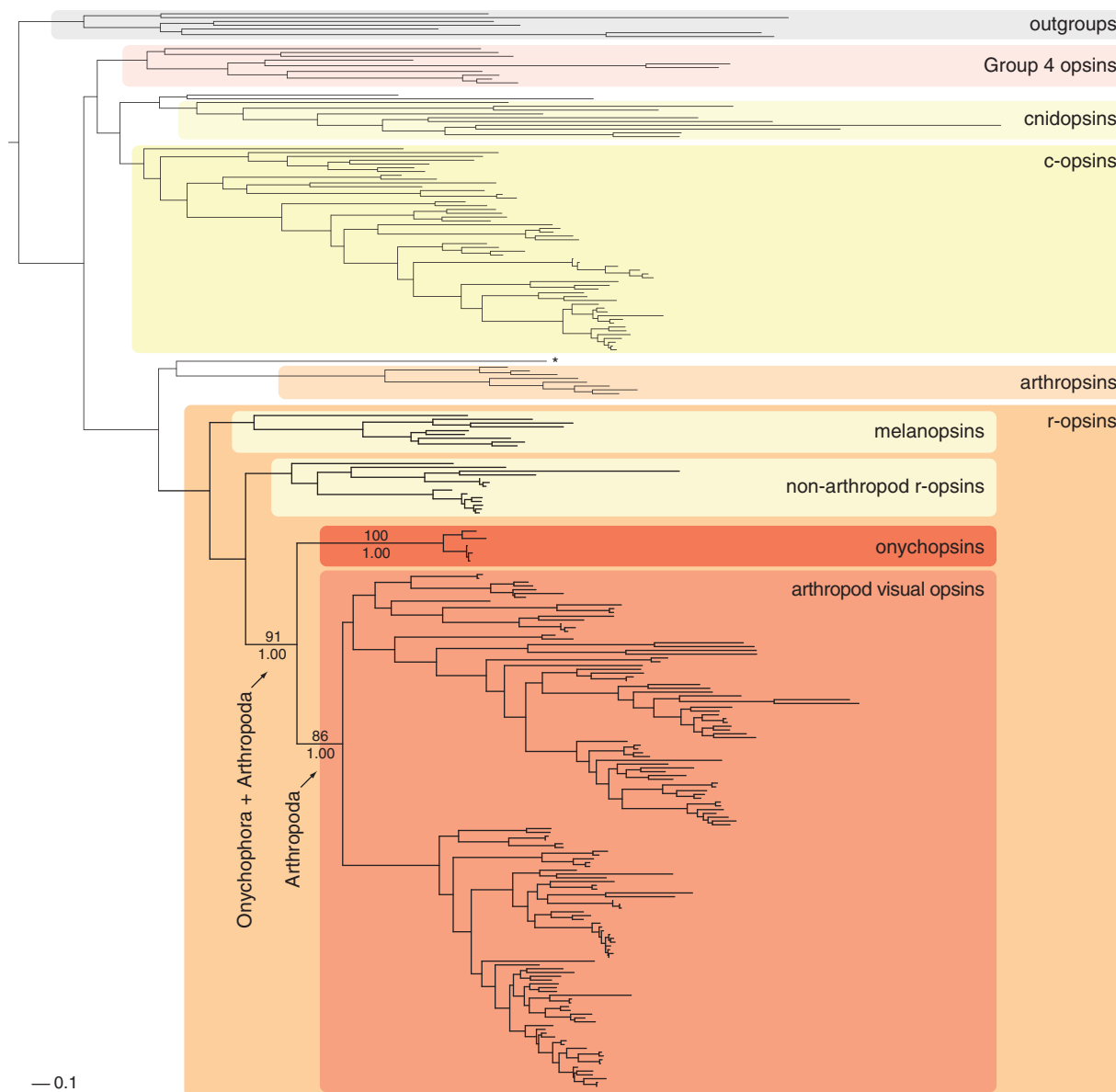
Fig. 2. Maximum likelihood tree of opsin subfamilies and position of the onychophoran opsin (onychopsin). Selected bootstrap values (1,000 replicates) from a ML-analysis using RAxML v7.2.8 (Stamatakis 2006) under the LG+I+G+F model of amino acid sequence evolution and posterior probabilities of Bayesian inference (Bpp) under the WAG+I+G model are provided at major nodes (ML/Bpp). G-protein-coupled receptor sequences other than opsins were used as outgroups. Asterisk indicates the position of an uncharacterized opsin from amphioxus, which forms the sister group to the enigmatic "arthropsins" with unknown function found in the genome of *Daphnia pulex* (water flea) (Colbourne et al. 2011). Group 4 opsins represent a mixed assemblage of RGRs, peropsins, and neuropsins, following the classification of Porter et al. (2012). Scale bar represents the number of substitutions per site. For a detailed version of the tree, with all taxon names, node support values, and GenBank accession numbers, see supplementary figures S4 and S5, Supplementary Material online.

in the center of the arena. A black cardboard box with a small opening for the body profile was placed over the frontal half of the animal to prevent light stimuli from reaching the eyes. In tests, the animal's rear half was illuminated by bright white light ($>10^{14}$ quanta cm^{-2} s^{-2}) from the xenon arc lamp by the UV-VIS-transmitting light guide. In controls, no light was presented. All experiments were recorded with an infrared-sensitive camera. The time the animal took to retract completely into the cardboard box was obtained from the video sequences and used as a measure for a possible light reaction mediated by extraocular photoreceptors.

Results and Discussion

Deep Transcriptome Sequencing Reveals a Single Opsin Gene in Onychophora

To determine the number and type of opsins in Onychophora, we performed deep transcriptome sequencing of dissected eyes and heads from specimens of the two major onychophoran subgroups, Peripatidae and Peripatopsidae, which diverged before the break-up of Gondwana over 175 million years ago (Allwood et al. 2010). We analyzed libraries from various embryonic stages and several adult tissues,
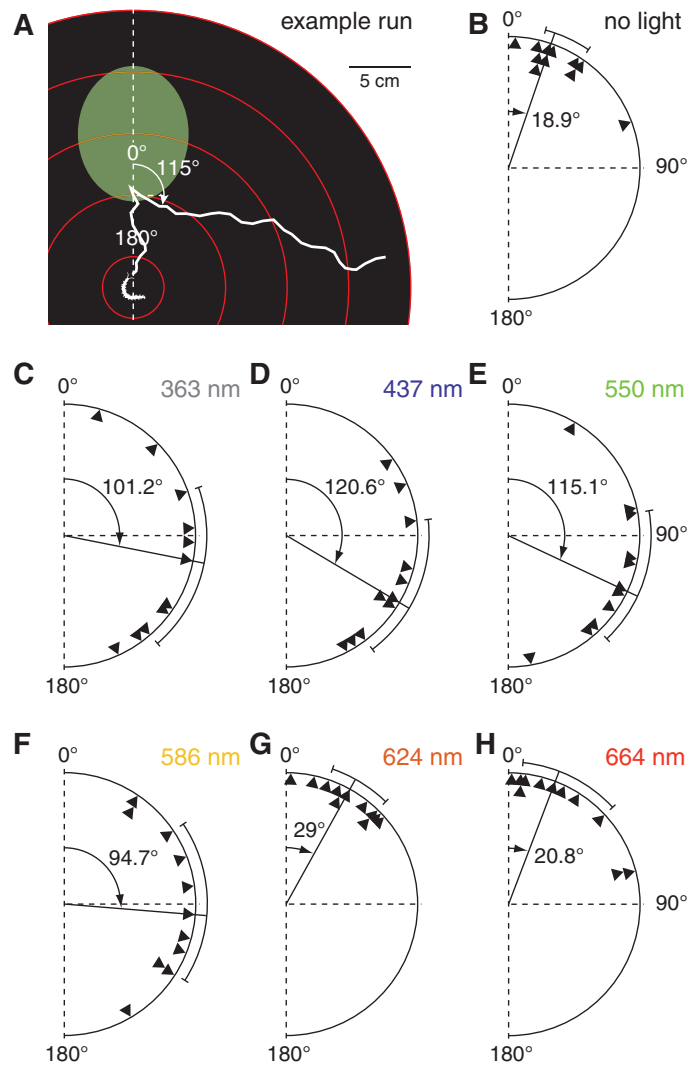
FIG. 3. Negative phototaxis in the onychophoran *Epiperipatus* cf. *isthmicola* in response to monochromatic light. (*A*) Example path (white line) of an animal released in the center of the circular arena and stimulated with green light, as seen from above. The strength of negative phototaxis was measured as the angular deviation of the animal (arrowed white arc) from its original moving direction 2.5 cm after stimulus onset. (*B–H*) Triangles show the absolute value of the angular deviation of 11 individuals in control runs (no light) and after exposure to ultraviolet, blue, green, yellow, orange, or red light. The solid black line denotes the median and the arc the interquartile range of the results.

including "eyes-only" libraries from two onychophoran species (*Euperipatoides rowelli*, *Epiperipatus* cf. *isthmicola*) and head libraries from three additional onychophoran species (*Phallocephale tallagandensis*, *Ooperipatus hispidus*, and *Eoperipatus* sp.). Altogether, for the deepest datasets (using Filter15), we assembled 123,903,469 sequence reads from *Euperipatoides rowelli* (~9.27 GB in total), 119,130,093 reads from *Epiperipatus* cf. *isthmicola* (~8.92 GB), 32,101,553 reads from *Phallocephale tallagandensis* (~2.44 GB), 33,827,778 reads from *Ooperipatus hispidus* (~2.57 GB), and 40,075,118 reads from *Eoperipatus* sp. (~3.04 GB). Moreover, we trimmed the raw data at two additional levels of stringency (Filter25, Filter30) to maximize the probability of detecting all expressed opsin genes in our transcriptome libraries (supplementary table S1, Supplementary Material online) as the read quality can be crucial for the assembly and read mapping (Minoche et al. 2011; Salzberg et al. 2012).

Using our deep sequencing approach, including adult and embryonic stages, we identified a single r-opsin ortholog ("onychopsin"; GenBank: JN661372, JN661373, JQ780371, JQ780372 and JQ780373) in each species studied. Notably, there is no evidence of other opsin genes or related receptors, such as "retinal G-protein coupled receptors" (RGRs), peropsins, neuropsins (Group 4 opsins *sensu* Porter et al. 2012), or c-type opsins, neither in the flat-filtered dataset (Filter15) nor in the more stringent filtered datasets (Filter25 and Filter30), in any of the five onychophoran species studied. Unfortunately, the onychophoran genomes are difficult to access for opsin screening because of their size (around twice the human genome; http://www.genomesize.com). However, irrespective of whether additional, nonfunctional opsins are present in the onychophoran genome, our deep sequencing approach and careful screening for opsin transcripts suggest that only a single opsin protein is expressed

in each onychophoran species studied. Taken together, these findings indicate a function of the identified opsins in vision, whereas they provide no evidence of additional functional opsin genes in Onychophora.

Phylogenetic Analyses Suggest Extensive Diversification of Visual r-Opsins in the Arthropod Lineage

Our results raise the question of whether only a single visual pigment was present in the last common ancestor of Onychophora and Arthropoda or, alternatively, whether the ancestral set of multiple opsin genes was reduced secondarily in Onychophora. To decide between these two alternatives, we performed a phylogenetic analysis of various opsin sequences from onychophorans, arthropods, and other bilaterian taxa. The obtained topology reveals strong support for the sister group relationship of the onychopsins with the visual r-opsins of arthropods (fig. 2 and supplementary figs. S3–S5, Supplementary Material online). The onychopsins and the visual arthropod r-opsins form two well-supported, reciprocally monophyletic sister clades. This is an important result for two reasons. First, reciprocal monophyly of these genes supports the sister-group status of the Onychophora and Arthropoda, a relationship that, although widely accepted, has been challenged (Ballard et al. 1992; Strausfeld, Strausfeld, Loesel, et al. 2006). We regard the alternative hypothesis of loss of one or more r-opsin gene copies in onychophorans to be unlikely as this would predict that the onychopsin sequence should be nested within the visual r-opsin clade from arthropods. Second, it is indicative of an extensive diversification of the r-opsin gene family in arthropods, following their divergence from Onychophora.

Behavioral Experiments Indicate Maximum Sensitivity of the Onychopsin to Blue–Green Light

To assess the spectral sensitivity of the onychopsin, we performed behavioral experiments exploiting the negative phototaxis of onychophorans (fig. 3A–H and supplementary movie S1, Supplementary Material online) (Monge-Nájera et al. 1993). Specimens of *Epiperipatus* cf. *isthmicola* react to monochromatic light of 363 nm (ultraviolet), 437 nm (blue to the human eye), 550 nm (green), and 586 nm (yellow) by significantly changing their walking direction (fig. 3C–F). In response to light of 624 nm (orange) and 664 nm (red), they continue walking straight, as in controls without light (fig. 3B, G, and H), thus indicating that they are unable to detect light of these long wavelengths ($n = 11$, p_{363}, p_{437}, p_{550} and $p_{586} < 0.05$, $p_{624} = 0.564$ and $p_{664} = 0.984$, Wilcoxon signed-rank tests with Dunn-Sidák correction for multiple comparisons). This finding is consistent with previous observations that onychophorans did not avoid dim red light, in contrast to daylight (Manton 1938; Alexander 1957; Hendrickson 1957). We can rule out that our animals avoided heat instead of light, because heat radiation was blocked by the narrowband interference filters we used to produce the monochromatic stimuli.

In a second set of experiments, we exclude that negative phototaxis in *Epiperipatus* cf. *isthmicola* is mediated by extraocular photoreceptors, such as LITE-1 (Edwards et al. 2008; Ward et al. 2008; Liu et al. 2010; Xiang et al. 2010). If the rear half of an animal is illuminated by bright white light, whereas the frontal half of the animal is shielded from light by a black cardboard box, the animal does not retract more quickly into the cardboard box than in controls, which were performed in complete darkness ($n = 11$; mean ± standard deviation of retraction time: 38.6 ± 33.5 s in tests and 36.0 ± 22.3 s in controls; no significant difference: paired t-test: $t_{10} = 0.31$, $P = 0.77$). In our experiments, the light intensities were lower than those used to study extraocular photoreception in *Drosophila melanogaster* (Xiang et al. 2010) and *Caenorhabditis elegans* (Ward et al. 2008). The intensities in these studies killed the animals after a few minutes. However, our white light stimulus was brighter (comprised more quanta) at any wavelength than the monochromatic stimuli in the behavioral experiments described above, that is, it should have elicited negative phototaxis if extraocular photoreceptors were involved. Moreover, neither putative *lite-1* nor *Gr28b* homologs, members of the gustatory receptor (*Gr*) family which are required for extraocular phototransduction in *Caenorhabditis elegans* and *Drosophila melanogaster* (Edwards et al. 2008; Liu et al. 2010; Xiang et al. 2010), are present in our transcriptome libraries, again providing no evidence of extraocular photodetection in the onychophoran species studied.

Considering the spectral sensitivity of negative phototaxis in *Epiperipatus* cf. *isthmicola* and the finding of only one expressed opsin in all five onychophoran species studied, we estimate that the onychopsin-based visual pigment of *Epiperipatus* cf. *isthmicola* is maximally sensitive to blue–green light (fig. 4). We use an established pigment absorbance template (Stavenga et al. 1993) and refer to conservative behavioral thresholds for this assessment. The animals showed negative phototaxis at 586 nm but not at 624 nm. If we suppose that the visual pigment still has 1% of its maximal absorbance at 586 nm, we obtain a lower limit for the peak absorbance at 481 nm; 1% is an arbitrary value for a behavioral threshold, but even a threshold of 0.01% does not shift the lower limit below 450 nm (i.e., it is still in the blue spectral range). The animals responded to 363 nm but not to 624 nm. A conservative estimate of the upper limit can thus be obtained by assuming that the absorbance of the visual pigment at 624 nm must be lower than at 363 nm. That way we receive 481 nm and 556 nm as conservative estimates for the lower and upper limits of the peak absorbance (fig. 4). The scatter in the behavioral response of the animals does not allow us to detect gradual differences in the sensitivity of the pigment across its absorption range from the ultraviolet to ~600 nm (fig. 4). For this purpose, electrophysiological recordings will be necessary. However, it is unlikely that the detected opsins belong to an ultraviolet opsin clade. It has been demonstrated previously that the presence of a lysine (K) amino acid at the position homologous to G^{90} of the bovine rhodopsin (Palczewski et al. 2000) is a prerequisite for ultraviolet-tuning properties of arthropod opsins: this is the case in all UV-opsins
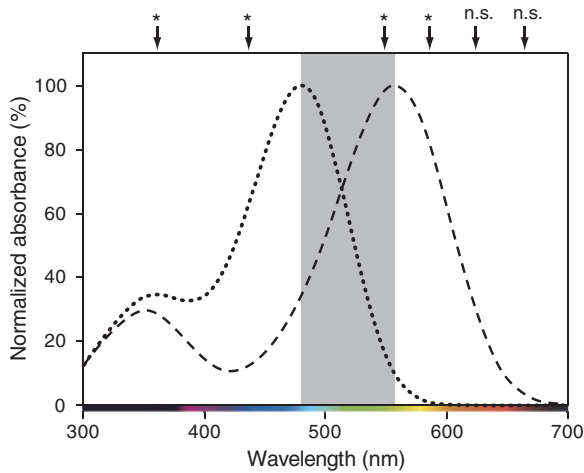
Fig. 4. Normalized absorbance spectra of visual pigments in Onychophora that can explain the results of behavioral experiments. Considering the spectral sensitivity of negative phototaxis in *Epiperipatus* cf. *isthmicola* and the finding of only one expressed opsin, the plotted curves give conservative estimates for the lower (dotted line) and upper limits (dashed line) of an opsin-based visual pigment. The wavelength of peak absorbance of the true pigment must be located between 481 and 556 nm (gray area), i.e., it is most sensitive to blue–green light. Arrows indicate the wavelengths that were tested behaviorally and the symbols above state whether the reactions were significantly different from controls (*significantly different with $P < 0.05$; n.s. = nonsignificant). Absorbance spectra were calculated using the template formulae developed by Stavenga et al. (1993).

of arthropods studied thus far (Salcedo et al. 2003; Koyanagi et al. 2008; Kashiyama et al. 2009). In accordance with the behavioral results, our sequence data suggest that the identified onychopsins might not form visual pigments maximally sensitive to ultraviolet light as they have asparagine (N) instead of lysine (K) at this position (supplementary fig. S6, Supplementary Material online).

Evidence for Monochromatic Vision in the Arthropod Lineage

Taken together, our molecular data support the assumption of monochromatic vision in Onychophora, and our behavioral data indicate a maximum sensitivity of the onychopsin to blue–green light. On the basis of our analyses, we suggest that the last common ancestor of Onychophora and Arthropoda possessed only one visual opsin gene and that the duplication and subsequent diversification of r-opsins (e.g., Briscoe 2000; Porter et al. 2007; Koyanagi et al. 2008; review Porter et al. 2012) occurred in arthropods, after their divergence from Onychophora. Thus, the origin of the multiple arthropod visual pigments and color vision corresponds with the evolution of compound eyes, which evolved in the arthropod lineage (Mayer 2006; Paterson et al. 2011). It also follows that the Cambrian stem-lineage (pan)arthropods without compound eyes, such as *Miraluolishania haikouensis* (Schoenemann et al. 2009; Legg et al. 2011), had no color vision.

Supplementary Material

Supplementary tables S1 and S2, figures S1–S6, and movie S1 are available at *Molecular Biology and Evolution* online (http://www.mbe.oxfordjournals.org/).

References

Akaike H. 1973. Information theory and an extension of the maximum likelihood principle. In: Petrov BN, Csaki F, editors. Second international symposium on information theory. Japan: Akademiai Kiado. p. 267–281.

Alexander AJ. 1957. Notes on onychophoran behavior. *Ann Natl Museum.* 14:35–43.

Allwood J, Gleeson D, Mayer G, Daniels S, Beggs JR, Buckley TR. 2010. Support for vicariant origins of the New Zealand Onychophora. *J Biogeogr.* 37:669–681.

Altschul SF, Madden TL, Schäffer AA, Zhang J, Zhang Z, Miller W, Lipman DJ. 1997. Gapped BLAST and PSI-BLAST: a new generation of protein database search programs. *Nucleic Acids Res.* 25:3389–3402.

Arendt D. 2003. Evolution of eyes and photoreceptor cell types. *Int J Develop Biol.* 47:563–571.

Arendt D, Wittbrodt J. 2001. Reconstructing the eyes of Urbilateria. *Philos Trans R Soc Lond B Biol Sci.* 356:1545–1563.

Baer A, Mayer G. 2012. Comparative anatomy of slime glands in Onychophora (velvet worms). *J Morphol.* Advance Access published June 18, 2012, doi:10.1002/jmor.20044

Ballard J, Olsen G, Faith D, Odgers W, Rowell D, Atkinson P. 1992. Evidence from 12S ribosomal RNA sequences that onychophorans are modified arthropods. *Science* 258:1345–1348.

Batschelet E. 1981. Circular statistics in biology. London: Academic Press.

Briscoe AD. 2000. Six opsins from the butterfly *Papilio glaucus*: molecular phylogenetic evidence for paralogous origins of red-sensitive visual pigments in insects. *J Mol Evol.* 51:110–121.

Briscoe AD, Chittka L. 2001. The evolution of color vision in insects. *Ann Rev Entomol.* 46:471–510.

Campbell LI, Rota-Stabelli O, Edgecombe GD, Marchioro T, Longhorn SJ, Telford MJ, Philippe H, Rebecchi L, Peterson KJ, Pisani D. 2011. MicroRNAs and phylogenomics resolve the relationships of Tardigrada and suggest that velvet worms are the sister group of Arthropoda. *Proc Natl Acad Sci U S A.* 108:15920–15924.

Colbourne JK, Pfrender ME, Gilbert D, et al. (69 co-authors). 2011. The ecoresponsive genome of *Daphnia pulex*. *Science* 331:555–561.

Darriba D, Taboada GL, Doallo R, Posada D. 2011. ProtTest 3: fast selection of best-fit models of protein evolution. *Bioinformatics* 27: 1164–1165.

Edgecombe G, Giribet G, Dunn C, Hejnol A, Kristensen R, Neves R, Rouse G, Worsaae K, Sørensen M. 2011. Higher-level metazoan relationships: recent progress and remaining questions. *Org Divers Evol.* 11:151–172.

Edwards SL, Charlie NK, Milfort MC, Brown BS, Gravlin CN, Knecht JE, Miller KG. 2008. A novel molecular solution for ultraviolet light detection in *Caenorhabditis elegans*. *PLoS Biol.* 6:e198.

Hendrickson J. 1957. *Peripatus* in Malaya. *Malayan Nat J.* 12:33–35.

Kashiyama K, Seki T, Numata H, Goto SG. 2009. Molecular characterization of visual pigments in Branchiopoda and the evolution of opsins in Arthropoda. *Mol Biol Evol.* 26:299–311.

Katoh K, Misawa K, Kuma Ki, Miyata T. 2002. MAFFT: a novel method for rapid multiple sequence alignment based on fast Fourier transform. *Nucleic Acids Res.* 30:3059–3066.

Katti C, Kempler K, Porter ML, Legg A, Gonzalez R, Garcia-Rivera E, Dugger D, Battelle BA. 2010. Opsin co-expression in *Limulus* photoreceptors: differential regulation by light and a circadian clock. *J Exp Biol.* 213:2589–2601.

Kircher M, Heyn P, Kelso J. 2011. Addressing challenges in the production and analysis of Illumina sequencing data. *BMC Genom.* 12:382.

Kircher M, Sawyer S, Meyer M. 2012. Double indexing overcomes inaccuracies in multiplex sequencing on the Illumina platform. *Nucleic Acids Res.* 40:e3.

Kircher M, Stenzel U, Kelso J. 2009. Improved base calling for the Illumina Genome Analyzer using machine learning strategies. *Genome Biol.* 10:R83.

Koyanagi M, Nagata T, Katoh K, Yamashita S, Tokunaga F. 2008. Molecular evolution of arthropod color vision deduced from multiple opsin genes of jumping spiders. *J Mol Evol.* 66:130–137.

Legg DA, Ma XY, Wolfe JM, Ortega-Hernandez J, Edgecombe GD, Sutton MD. 2011. Lobopodian phylogeny reanalysed. *Nature* 476:E2–E3.

Lehmann T, Heß M, Melzer RR. 2012. Wiring a periscope—ocelli, retinula axons, visual neuropils and the ancestrality of sea spiders. *PLoS One* 7:e30474.

Letunic I, Bork P. 2011. Interactive Tree Of Life v2: online annotation and display of phylogenetic trees made easy. *Nucleic Acids Res.* 39: W475–W478.

Liu J, Ward A, Gao J, et al. (13 co-authors). 2010. *C. elegans* phototransduction requires a G protein-dependent cGMP pathway and a taste receptor homolog. *Nat Neurosci.* 13:715–722.

Ma X, Hou X, Aldridge RJ, Siveter DJ, Siveter DJ, Gabbott SE, Purnell MA, Parker AR, Edgecombe GD. 2012. Morphology of Cambrian lobopodian eyes from the Chengjiang Lagerstätte and their evolutionary significance. *Arthropod Struct Develop.* Advance Access published April 4, 2012, doi:10.1016/j.asd.2012.03.002

Manton SM. 1938. Studies on the Onychophora—VI. The life-history of *Peripatopsis*. *Ann Mag Nat Hist.* 11:515–529.

Mayer G. 2006. Structure and development of onychophoran eyes: what is the ancestral visual organ in arthropods? *Arthropod Struct Develop.* 35:231–245.

Meyer M, Kircher M. 2010. Illumina sequencing library preparation for highly multiplexed target capture and sequencing. *Cold Spring Harb Protoc.* 2010:pdb.prot5448.

Minoche AE, Dohm JC, Himmelbauer H. 2011. Evaluation of genomic high-throughput sequencing data generated on Illumina HiSeq and Genome Analyzer systems. *Genome Biol.* 12:R112.

Monge-Nájera J, Barrientos Z, Aguilar F. 1993. Behavior of *Epiperipatus biolleyi* (Onychophora: Peripatidae) under laboratory conditions. *Revista de Biol Trop.* 41:689–696.

Palczewski K, Kumasaka T, Hori T, et al. (12 co-authors). 2000. Crystal structure of rhodopsin: a G protein-coupled receptor. *Science* 289: 739–745.

Passameneck Y, Furchheim N, Hejnol A, Martindale M, Luter C. 2011. Ciliary photoreceptors in the cerebral eyes of a protostome larva. *EvoDevo.* 2:6.

Paterson JR, Garcia-Bellido DC, Lee MSY, Brock GA, Jago JB, Edgecombe GD. 2011. Acute vision in the giant Cambrian predator *Anomalocaris* and the origin of compound eyes. *Nature* 480: 237–240.

Plachetzki DC, Degnan BM, Oakley TH. 2007. The origins of novel protein interactions during animal opsin evolution. *PLoS One* 2:e1054.

Porter ML, Blasic JR, Bok MJ, Cameron EG, Pringle T, Cronin TW, Robinson PR. 2012. Shedding new light on opsin evolution. *Proc Roy Soc B Biol Sci.* 279:3–14.

Porter ML, Cronin TW, McClellan DA, Crandall KA. 2007. Molecular characterization of crustacean visual pigments and the evolution of pancrustacean opsins. *Mol Biol Evol.* 24:253–268.

Ronquist F, Huelsenbeck JP. 2003. MrBayes 3: Bayesian phylogenetic inference under mixed models. *Bioinformatics* 19:1572–1574.

Salcedo E, Zheng L, Phistry M, Bagg EE, Britt SG. 2003. Molecular basis for ultraviolet vision in invertebrates. *J Neurosci.* 23:10873–10878.

Salzberg SL, Phillippy AM, Zimin A, et al. (13 co-authors). 2012. GAGE: a critical evaluation of genome assemblies and assembly algorithms. *Genome Res.* 22:557–567.

Schoenemann B, Liu J-N, Shu D-G, Han J, Zhang Z-F. 2009. A miniscule optimized visual system in the Lower Cambrian. *Lethaia* 42:265–273.

Shichida Y, Imai H. 1998. Visual pigment: G-protein-coupled receptor for light signals. *Cell Mol Life Sci.* 54:1299–1315.

Shichida Y, Matsuyama T. 2009. Evolution of opsins and phototransduction. *Philos Trans Roy Soc B Biol Sci.* 364:2881–2895.

Stamatakis A. 2006. RAxML-VI-HPC: maximum likelihood-based phylogenetic analyses with thousands of taxa and mixed models. *Bioinformatics* 22:2688–2690.

Stavenga DG, Smits RP, Hoenders BJ. 1993. Simple exponential functions describing the absorbance bands of visual pigment spectra. *Vision Res.* 33:1011–1017.

Strausfeld NJ, Strausfeld CM, Loesel R, Rowell D, Stowe S. 2006. Arthropod phylogeny: onychophoran brain organization suggests an archaic relationship with a chelicerate stem lineage. *Proc Roy Soc B Biol Sci.* 273:1857–1866.

Strausfeld NJ, Strausfeld CM, Stowe S, Rowell D, Loesel R. 2006. The organization and evolutionary implications of neuropils and their neurons in the brain of the onychophoran *Euperipatoides rowelli*. *Arthropod Struct Dev.* 35:169–196.

Suga H, Schmid V, Gehring WJ. 2008. Evolution and functional diversity of jellyfish opsins. *Curr Biol.* 18:51–55.

Vopalensky P, Kozmik Z. 2009. Eye evolution: common use and independent recruitment of genetic components. *Philos Trans Roy Soc B Biol Sci.* 364:2819–2832.

Ward A, Liu J, Feng Z, Xu XZS. 2008. Light-sensitive neurons and channels mediate phototaxis in *C. elegans*. *Nat Neurosci.* 11:916–922.

Xiang Y, Yuan Q, Vogt N, Looger LL, Jan LY, Jan YN. 2010. Light-avoidance-mediating photoreceptors tile the *Drosophila* larval body wall. *Nature* 468:921–926.